Chemical Engineering Journal 165 (2010) 597–606

Contents lists available at ScienceDirect

Chemical Engineering Journal

journal homepage: www.elsevier.com/locate/cej

# Development of experimental design models to predict Photo-Fenton oxidation of a commercially important naphthalene sulfonate and its organic carbon content

Idil Arslan-Alaton*, Arzu Betul Yalabik, Tugba Olmez-Hanci

*Istanbul Technical University, Faculty of Civil Engineering, Department of Environmental Engineering, 34469 Maslak, Istanbul, Turkey*

ARTICLE INFO

*Article history:*
Received 24 June 2010
Received in revised form
30 September 2010
Accepted 1 October 2010

*Keywords:*
Naphthalene sulfonates
K-acid
Advanced oxidation processes
Photo-Fenton treatment
Response surface methodology
Central composite design

ABSTRACT

In the present study, Photo-Fenton oxidation of the commercially important K-acid (2-naphthylamine-3,6,8-trisulfonic acid) was optimized and modeled by employing response surface methodology and central composite design. The experimental design tool was used to assess the influence of treatment time ($t_r$), initial COD of aqueous K-acid solutions ($COD_o$) as well as $H_2O_2$ and $Fe^{2+}$ concentrations on K-acid, COD and TOC removal efficiencies. According to the established second-order polynomial regression models, K-acid removal efficiency was affected by the process variables in the following decreasing order; $t_r$ > $COD_o$ (negative impact) > $Fe^{2+}$ > $H_2O_2$, while the effect on COD and TOC removals was $COD_o$ (negative impact) > $H_2O_2$ > $t_r$ > $Fe^{2+}$. Analysis of variance indicated that the experimental design models obtained for the Photo-Fenton oxidation of aqueous K-acid and its organic carbon content (expressed as COD and TOC) were statistically significant and satisfactorily described the treatment process for the entire Photo-Fenton treatment period (up to 125 min) as well as different treatment targets (partial and full oxidation) and initial COD values (150–750 mg/L). Complete K-acid removal accompanied with high COD (70–100%) and TOC (55–100%) abatements were achieved under relatively mild Photo-Fenton treatment conditions.



## 1. Introduction

Naphthalene sulfonates are used as solubilizing and dispersing agents in a wide range of industrial product formulations including optical brighteners, pesticides, ion exchange resins, pharmaceuticals and plasticizers [1]. Besides, naphthalene sulfonates including H-acid, J-acid and K-acid are naphthylamine sulfonic acid derivatives being frequently used in textile dye manufacture and hence their production is of considerable economic importance. From the environmental point of view, the fate of naphthalene sulfonates and their metabolites in biological treatment plants and aquatic ecosystems is still not very clear since until now only limited attention has been paid towards their occurrence and degradability in engineered treatment systems as well as in the natural environment [2–4]. The presence of at least one sulfonated group ($-SO_3^-$) makes these compounds very resistant towards oxidative attack, highly water soluble and mobile. Hence, after production and application in different industrial sectors, naphthalene sulfonates easily enter the aquatic environment and do not significantly sorb onto sediments and/or soil [5]. Due to the fact that conventional biological, physical and chemical treatment methods are not very effective in the removal of naphthalene sulfonates, alternative options have to be considered and evaluated.

Among chemical oxidation methods, advanced oxidation processes (AOPs) have been successfully employed for the degradation of toxic and/or recalcitrant pollutants found in water or wastewater originating from different industries [6,7]. These processes involve the in situ generation of free radicals (mainly $HO^{\cdot}$) that violently and almost indiscriminately react with most organic pollutants. Recently we could demonstrate that commercially important naphthalene sulfonic acids can be treated efficiently with AOPs including $H_2O_2$/UV-C [8] and near UV-light assisted Photo-Fenton-like ($Fe^{3+}$/$H_2O_2$/UV-A) oxidation systems [9]. However, these studies indicated that for efficient $H_2O_2$/UV-C treatment, long reaction periods and/or high $H_2O_2$ concentrations are required, and Fenton's reagent applied in the presence of long-UV (UV-A) irradiation results in incomplete degradation of target pollutant to intermediate oxidation products. On the other hand, Photo-Fenton oxidation in the presence of short-UV (UV-C) light enables a more thorough and fast oxidation as a consequence of the higher quantum yields achieved under irradiation of ferric hydroxo complexes at these wavelengths [10–12]. Besides, in the presence of UV-C light, $H_2O_2$ also photolyzes thus additionally contributing to $HO^{\cdot}$ formation during Photo-Fenton treatment [13,14].

* Corresponding author. Tel.: +90 212 285 37 86; fax: +90 212 285 65 45.
*E-mail address:* arslanid@itu.edu.tr (I. Arslan-Alaton).

1385-8947/$ – see front matter © 2010 Elsevier B.V. All rights reserved.
doi:10.1016/j.cej.2010.10.003

**Nomenclature**

*List of abbreviations and symbols*

| | |
|---|---|
| ANOVA | analysis of variance |
| AOPs | advanced oxidation processes |
| CCD | central composite design |
| COD | chemical oxygen demand (mg/L) |
| $COD_o$ | initial COD (mg/L) |
| DAD | diode-array detector |
| *F*-Value | Fisher value |
| FO | full oxidation (mineralization) |
| $HO^{\cdot}$ | hydroxyl radical (s) |
| $H_2O_2$ | hydrogen peroxide (mg/L) |
| HPLC | high performance liquid chromatography |
| ISO | International Standardization Organization |
| PO | partial oxidation |
| Prob | probability |
| $R^2$ | coefficient of variation |
| RSM | response surface methodology |
| TOC | total organic carbon (mg/L) |
| $t_r$ | photocatalytic treatment time (min) |
| UV | ultra violet |
| WPCR | water pollution control regulation |

Several process parameters (reaction pH, photocatalytic treatment time, initial $Fe^{2+}$, $H_2O_2$ and pollutant concentrations) affect Photo-Fenton treatment efficiency and may interact with each other [15–19]. Consequently, process optimization using a single-factor-at-a-time approach (varying one process variable thereby keeping the others constant) can be very time consuming, and does not consider that not only single, but also binary effects are involved. In particular for treatment processes having an extremely complex reaction pathway a more suitable optimization approach is to employ multivariate analysis. Response surface methodology (RSM) is a powerful mathematical and statistical design tool that can be used to evaluate, model and optimize the performance of complex systems by considering the relative significance of several factors even in the presence of complicated, multi-dimensional interactions [20–22]. Several studies have reported the individual and interactive effects of process variables influencing the Photo-Fenton or Fenton processes and observed similar relationships for different industrial effluents as well as single model pollutants. As far as we are concerned, no experimental and statistical design procedures have been employed until now to model and optimize the Photo-Fenton oxidation of naphthalene sulfonates by setting economically and technically acceptable treatment goals under varying reaction conditions including initial pollutant concentrations considering that the concentration of naphthalene sulfonates can differ appreciably from point source to point source. Apparently, treatment of K-acid-bearing industrial effluent at source where it is present in its most concentrated form is a convenient solution. In the present work the main parameters affecting the treatment performance of the Photo-Fenton process and the relative intensity of each investigated parameter on the treatment efficiency was evaluated by the RSM-central composite design (CCD) tool to improve the common knowledge and database in this area. It was also taken into account that treatment conditions may vary for the removal of parent pollutant and its degradation products that are usually collectively presented with the environmental sum parameters COD and TOC. K-acid (2-naphthylamine-3,6,8-tri sulfonic acid), a difficult-to-treat, commercially important dye precursor was selected as the index chemical to experimentally design, model and optimize the Photo-Fenton treatment of a refractory industrial pollutant. Two different experimental and statistical design matrices were developed for the assessment of both K-acid and its organic carbon content removals on the basis of treatment time. Process optimization was based on two Photo-Fenton treatment targets; (i) partial oxidation (for COD, TOC removals) to achieve complete parent pollutant abatement, abbreviated herein as "PO", and (ii) full treatment for complete oxidation (mineralization) of aqueous K-acid, indicated as "FO" throughout the paper. In the last part of the study, the fitness and significance of the developed RSM models were verified for different treatment times and targets.

## 2. Materials and methods

### 2.1. K-acid and other chemicals

The commercial-grade K-acid ($C_{10}H_9O_9S_3$; molecular weight: 383 g/mol; CAS: 118-03-6; purity: min 65%; appearance: yellowish moist powder; 0.63 mg COD/mg K-acid; 0.18 mg TOC/mg K-acid) was supplied by a local dye manufacturing plant and used as received without any further purification. Aqueous K-acid solutions were prepared in distilled water to attain different COD values in the range of 150–750 mg/L. 35% w/w $H_2O_2$ (Fluka, USA) was used as received without dilution. Residual $H_2O_2$ was destroyed with enzyme Catalase derived from *Micrococcus lysodeikticus* (100181 U/mL, Fluka, USA). The $Fe^{2+}$ source was prepared daily by dissolving $FeSO_4{\cdot}7H_2O$ (Fluka, USA) in distilled water to obtain a 10% (w/v) stock solution. Several concentrations of $HNO_3$ (Merck, Germany) and NaOH (Merck, Germany) solutions were used for pH adjustment. HPLC-grade acetonitrile ($CH_3CN$) was used as the mobile phase in the HPLC measurements (Merck, Germany). All other reagents were of analytical grade.

### 2.2. Photo-Fenton experiments

$H_2O_2$/UV-C (dark) Fenton control and Photo-Fenton experiments were performed at varying K-acid (COD), $Fe^{2+}$ and $H_2O_2$ concentrations for a total treatment period of 125 min. All experiments were conducted at the initial pH of $3.0 \pm 0.1$, which is known as the optimum pH for Photo-Fenton oxidation [13]. The reaction pH and ionic strength of the aqueous K-acid solution was not controlled during the experiments. The UV-C photoreactor set-up was a 3250 mL-capacity batch stainless steel tube (length = 84.5 cm; width = 8.0 cm) bearing a 40 W low pressure, mercury vapor sterilization lamp that was located at the centre of the photoreactor in a quartz sleeve. The incident light flux of the UV-C lamp at 253.7 nm was determined via $H_2O_2$ actinometry [23] as $1.6 \times 10^{-5}$ einstein/(L × s). The effective UV-C light path length was found as 4.31 cm by the same analytical method. During a typical run, 3250 mL aqueous surfactant solution was continuously circulated through the reactor by means of a peristaltic pump (Meterpump Systems, Aripa) at a rate of 400 mL/min, corresponding to a hydraulic retention time of 8 min in the photoreactor.

### 2.3. Experimental design and statistical analysis

In the present study, a CCD methodology with four independent variables was applied to investigate the effect of the photocatalytic treatment time (coded as $X_1$), initial COD content (coded $X_2$), $H_2O_2$ (coded $X_3$) and $Fe^{2+}$ (coded $X_4$) concentrations on the Photo-Fenton ($Fe^{2+}/H_2O_2$/UV-C) oxidation of aqueous K-acid (Table 1). The CCD consisted of $2^4$ factorial points, eight axial points and two replicates of the central point resulting in a total number of 26 experiments. The K-acid ($Y_1$, %), COD ($Y_2$, %) and TOC ($Y_3$, %) removal efficiencies were selected as the responses (dependent process variables) to assess the Photo-Fenton treatment process. As being expected

**Table 1**
Levels and ranges of selected process independent variables in terms of real and coded factors.

| Process independent variables | Codes | Real values of code levels | | | | |
|---|---|---|---|---|---|---|
| | | −2 | −1 | 0 | 1 | 2 |
| Treatment time (min) | $X_{1-K}$ | 10 | 20 | 30 | 40 | 50 |
| | $X_{1-O}$ | 25 | 50 | 75 | 100 | 125 |
| Initial COD (mg/L) | $X_2$ | 150 | 300 | 450 | 600 | 750 |
| Initial $H_2O_2$ (mM) | $X_3$ | 10 | 20 | 30 | 40 | 50 |
| Initial $Fe^{2+}$ (mM) | $X_4$ | 0.2 | 0.4 | 0.6 | 0.8 | 1.0 |

for photochemical AOPs [24], the degradation of the original (parent) pollutant is usually faster than that of its oxidation products, which are typically expressed in terms of the collective parameters COD and TOC. Hence, due to the differences between parent compound (K-acid) and organic matter (COD, TOC) abatement rates, two different ranges were selected for the independent process variable "treatment time – $t_r$" ($X_1$) based on our preliminary studies to model K-acid ($X_{1-K}$) and organic matter ($X_{1-O}$) removal efficiencies. The range and central point values of these four independent process variables were based on the results of our previous studies [9,18]. Experimental runs were randomized to minimize the effects of unexpected variations in the observed responses.

Table 2 shows the actual values of the independent variables at which the experiments were conducted to estimate the response variables % K-acid ($Y_1$), COD ($Y_2$) and TOC ($Y_3$) removals. Each response was used to develop an empirical model which correlated the process responses to the four process independent variables. The general equation of the second-order polynomial regression model is presented in Eq. (1) given below [22];

$$Y(\%) = b_o + \sum b_i X_i + \sum b_{ii} X_i^2 + \sum b_{ij} X_i X_j \quad (1)$$

where $Y$ stands for the predicted responses (percent K-acid, COD and TOC removals), $b_o$ for the constant coefficient, $b_i$; $b_{ii}$ and $b_{ij}$ for the regression coefficients and $X_i$, $X_j$ indicate the levels of the process independent variables [22].

According to experimentally obtained results, response surface plots were developed using the Design Expert® Software (Version 7.1.6) from Stat-Ease Inc., USA, and represented a function of two independent variables while keeping the other independent variable(s) at the zero level. These response surface plots provided a visual interpretation of the interaction between two process variables. Multiple regression analysis carried out by the least squares method generates the analysis of variance (ANOVA) data for verification of the robustness of the models (95% confidence level). The adequacy of the model was checked by evaluating the lack of fit, coefficient of determination ($R^2$) and the Fisher test value ($F$-value) obtained from ANOVA [21,25–28]. The significances of all model terms in the polynomial equations were statistically examined by computing the $F$-value at a probability value (Prob > $F$) of 0.050. The optimum $Fe^{2+}/H_2O_2$/UV-C treatment conditions for K-acid and organic matter (COD, TOC) removals were estimated using the numerical and graphical optimization tool of Design Expert Software® at different initial CODs and two different treatment targets (FO and PO).

### 2.4. Analytical procedures

Samples were taken at regular time intervals for K-acid, COD, TOC, residual $H_2O_2$ and pH measurements. In order to prevent the positive interference of $H_2O_2$, prior to all COD analyses, the pH of each sample solution was adjusted to 6.5–7.5 and thereafter catalase enzyme was added to destroy any residual $H_2O_2$, whereas unreacted $H_2O_2$ was measured directly. K-acid abatement was monitored via HPLC (Agilent 1100 series, USA) equipped

**Table 2**
The experimental design for response surface analysis in terms of actual values.

| Experiment no. | $X_{1-K}$ | $X_{1-O}$ | $X_2$ | $X_3$ | $X_4$ |
|---|---|---|---|---|---|
| | $t_r$ (min) | | Initial COD (mg/L) | Initial $H_2O_2$ (mM) | Initial $Fe^{2+}$ (mM) |
| 1 | 20 | 100 | 600 | 40 | 0.4 |
| 2 | 40 | 50 | 600 | 20 | 0.4 |
| 3 | 20 | 100 | 300 | 20 | 0.4 |
| 4 | 30 | 75 | 450 | 50 | 0.6 |
| 5 | 40 | 100 | 300 | 40 | 0.4 |
| 6 | 30 | 75 | 750 | 30 | 0.6 |
| 7 | 30 | 75 | 150 | 30 | 0.6 |
| 8 | 20 | 50 | 300 | 40 | 0.4 |
| 9 | 20 | 50 | 600 | 20 | 0.8 |
| 10 | 30 | 75 | 450 | 30 | 1.0 |
| 11 | 30 | 25 | 450 | 30 | 0.6 |
| 12 | 50 | 75 | 450 | 30 | 0.6 |
| 13 | 20 | 50 | 300 | 20 | 0.8 |
| 14 | 20 | 100 | 300 | 40 | 0.8 |
| 15 | 40 | 50 | 600 | 40 | 0.4 |
| 16 | 20 | 100 | 600 | 20 | 0.4 |
| 17 | 40 | 100 | 300 | 20 | 0.8 |
| 18 | 20 | 50 | 600 | 40 | 0.8 |
| 19 | 10 | 125 | 450 | 30 | 0.6 |
| 20 | 40 | 50 | 300 | 40 | 0.8 |
| 21 | 30 | 75 | 450 | 30 | 0.6 |
| 22 | 30 | 75 | 450 | 10 | 0.6 |
| 23 | 30 | 75 | 450 | 30 | 0.2 |
| 24 | 40 | 100 | 600 | 20 | 0.8 |
| 25 | 40 | 50 | 300 | 20 | 0.4 |
| 26 | 40 | 100 | 600 | 40 | 0.8 |

with a diode array detector (DAD; λ = 310 nm) and a Novapack $C_{18}$ (Waters, USA) column. $CH_3CN/H_2O$ (60/40, v/v) was used as mobile phase for the analysis of the model pollutant (K-acid) at a flow rate of 1 mL/min. The column temperature was set as 30 °C for all measurements and the injection volume was selected as 30 μL. The instrument detection limit (1.5 mg/L) for K-acid was determined as the lowest injected standard that gave a signal-to-noise ratio of at least three and an accuracy of 80–95%. The limit of quantification was calculated as 10 times of the signal-to-noise ratio as 5 mg/L. The COD of untreated and photocatalytically treated samples were determined by the closed reflux titrimetric method in accordance with ISO 6060 [29]. The TOC content of the samples was monitored on a Shimadzu TOC $V_{PCN}$ carbon analyzer equipped with an autosampler. Residual (unreacted) $H_2O_2$ was traced by employing the molybdate-catalyzed iodometric method [30] during the course of reaction. Samples pH values were determined with an Orion 720$^+$ model pH-meter.

## 3. Results and discussion

### 3.1. Results of the Photo-Fenton and control experiments

Preliminary control experiments were performed at an initial K-acid COD of 450 mg/L that is an average, typical COD value for K-acid synthesis effluent, in the absence of $Fe^{2+}$ ($H_2O_2$/UV-C oxidation) and also without UV-C light irradiation (dark Fenton experiment) to elucidate the effect of $Fe^{2+}$ catalyst and UV-C light radiation on the advanced oxidation of aqueous K-acid solution. Changes in K-acid (a), COD (b) and TOC (c) values as a function of photocatalytic treatment time are depicted in Fig. 1 for the control as well as Photo-Fenton experiments. For these preliminary treatability studies, $H_2O_2$ (30 mM) and $Fe^{2+}$ (0.5 mM) concentrations were selected upon consideration of optimum $Fe^{2+}$: $H_2O_2$ molar ratios obtained in former related research work and our own experiences in similar case studies [8,9,18]. All experiments were conducted at a fixed pH value of 3 that is generally accepted as the optimum pH for iron-based AOPs [13].

From Fig. 1 it is evident that during the application of the selected AOPs, K-acid (parent compound) degradation is appreciably faster than the removal of the parameters COD and TOC. This is not surprising for the fact that K-acid degradation only relies on the oxidative cleavage of the original naphthalene ring, whereas organic matter removal occurs through a multi-stage consecutive free radical chain reactions that ultimately leads to the formation of low-molecular weight oxidation products, mineral acids and carbon dioxide [31,32].

As expected, the addition of $Fe^{2+}$ catalyst had a significant accelerating effect in terms of K-acid as well as COD and TOC abatement rates as compared with the $H_2O_2$/UV-C process. As can be concluded from Fig. 1(a), prolonged treatment times or alternatively, huge $H_2O_2$ concentrations would be required to completely degrade K-acid, the original pollutant, by the $H_2O_2$/UV-C process, since even after 120 min treatment K-acid removal is not more than 60% in the absence of $Fe^{2+}$. On the other hand, K-acid abatement was complete within 60 min treatment when Fenton and Photo-Fenton oxidation process were applied. Moreover, the COD and TOC parameters were only poorly removed via mere $H_2O_2$/UV-C treatment; TOC practically remained unchanged indicating that the originally present K-acid is converted to different advanced oxidation intermediates that cannot be effectively oxidized in the absence of $Fe^{2+}$ catalyst. From these findings it can be deduced that if solely K-acid degradation is aimed, its removal rate can be considerably enhanced upon $Fe^{2+}$ addition even without the necessity to apply additional UV-C light, e.g. via the classical Fenton's process.

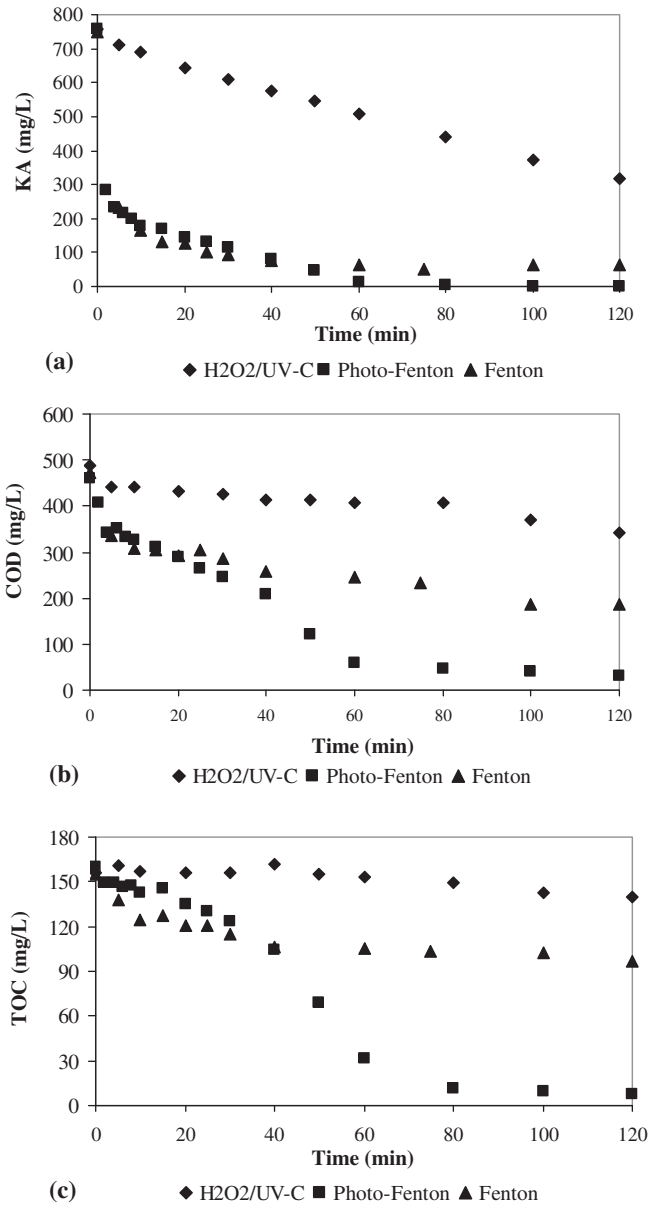


**Fig. 1.** K-acid (a), COD (b) and TOC (c) abatement rates observed during Photo-Fenton and control (dark Fenton, $H_2O_2$-UV-C) experiments. Experimental conditions: $COD_o$ = 450 mg/L; $H_2O_2$ = 30 mM and $Fe^{2+}$ = 0.5 mM for Fenton and Photo-Fenton processes; initial pH 3.0.

It can be followed from Fig. 1(b) and (c) that the positive influence of UV-C light irradiation on Fenton's reaction became evident in the later stages of the Photo-Fenton process with respect to organic matter removal (e.g. for the collective parameters COD and TOC). Fenton's reaction practically stopped after 40 min treatment, whereas in the presence of UV-C light further degradation took place until a treatment time of 80 min. $H_2O_2$ was totally consumed after 40 min treatment during both Photo-Fenton and Fenton reactions, coinciding with the termination of the dark Fenton process. As is well-known from Photo-Fenton's chemistry, in the presence of UV-C light the overall oxidation reaction is significantly enhanced due to the following reaction [13,14];

$$Fe(III)OH^{2+} + h\upsilon \rightarrow Fe^{2+} + HO^{\cdot} \quad (2)$$

Reaction (2) is not limited to the presence of UV-C light irradiation and may also be observed in the presence of long UV and even visible light, though with significant limitations since the reaction

**Table 3**
Experimentally obtained and predicted K-acid, COD and TOC removal efficiencies during Photo-Fenton oxidation process designed by the RSM-CCD tool.

| Experiment no. | K-acid removal ($Y_1$, %) | | COD removal ($Y_2$, %) | | TOC removal ($Y_3$, %) | |
|---|---|---|---|---|---|---|
| | Experimental | Predicted | Experimental | Predicted | Experimental | Predicted |
| 1 | 65 ± 3 | 68 | 85 ± 9 | 88 | 89 ± 9 | 90 |
| 2 | 80 ± 4 | 82 | 41 ± 4 | 36 | 22 ± 2 | 13 |
| 3 | 81 ± 4 | 80 | 82 ± 8 | 86 | 97 ± 3 | 100 |
| 4 | 93 ± 5 | 92 | 77 ± 8 | 81 | 95 ± 5 | 96 |
| 5 | 95 ± 5 | 100 | 98 ± 2 | 98 | 98 ± 2 | 100 |
| 6 | 77 ± 4 | 76 | 64 ± 6 | 62 | 42 ± 4 | 36 |
| 7 | 95 ± 5 | 100 | 95 ± 5 | 100 | 94 ± 6 | 100 |
| 8 | 87 ± 4 | 85 | 94 ± 6 | 83 | 92 ± 8 | 80 |
| 9 | 75 ± 4 | 76 | 54 ± 5 | 52 | 36 ± 4 | 29 |
| 10 | 93 ± 5 | 93 | 88 ± 9 | 97 | 91 ± 9 | 97 |
| 11 | 90 ± 5 | 90 | 50 ± 5 | 61 | 26 ± 3 | 43 |
| 12 | 95 ± 5 | 96 | 90 ± 9 | 90 | 84 ± 8 | 84 |
| 13 | 89 ± 4 | 88 | 97 ± 3 | 89 | 95 ± 5 | 92 |
| 14 | 93 ± 5 | 92 | 98 ± 2 | 99 | 95 ± 5 | 100 |
| 15 | 87 ± 4 | 86 | 55 ± 6 | 61 | 42 ± 4 | 49 |
| 16 | 70 ± 4 | 65 | 57 ± 6 | 58 | 41 ± 4 | 43 |
| 17 | 95 ± 5 | 98 | 95 ± 5 | 100 | 95 ± 5 | 100 |
| 18 | 81 ± 4 | 79 | 85 ± 9 | 77 | 74 ± 7 | 71 |
| 19 | 64 ± 3 | 68 | 90 ± 9 | 100 | 87 ± 9 | 100 |
| 20 | 95 ± 5 | 100 | 98 ± 2 | 96 | 95 ± 5 | 95 |
| 21 | 90 ± 5 | 90 | 90 ± 9 | 90 | 84 ± 8 | 84 |
| 22 | 81 ± 4 | 84 | 40 ± 4 | 43 | 31 ± 3 | 46 |
| 23 | 76 ± 4 | 78 | 83 ± 8 | 81 | 74 ± 7 | 79 |
| 24 | 88 ± 4 | 89 | 56 ± 6 | 62 | 40 ± 4 | 45 |
| 25 | 95 ± 5 | 95 | 75 ± 8 | 76 | 92 ± 8 | 83 |
| 26 | 92 ± 5 | 93 | 94 ± 6 | 92 | 92 ± 8 | 97 |

is a strong function of radiation wavelength. As also observed in the present work, the continuing COD and TOC abatements observed during the later stages of Photo-Fenton treatment resulted in the degradation of the formed reaction intermediates to oxidation end products and most probably due to Reaction (2). Moreover, the formation of photocatalytically active ferric-organo complexes (Fe-carboxylates) and organic radicals due to radical chain reactions involving molecular oxygen speculatively explain the progress of the oxidation progress during the reaction period between 40 min and 80 min of the Photo-Fenton process, where $H_2O_2$ was already depleted (totally consumed) and hence not available in the reaction medium [33].

Another interesting point that was observed during the preliminary control experiments was that during the early stages of K-acid treatment, TOC conversions obtained for the dark Fenton process were higher than those of the Photo-Fenton process. This retardation in TOC removal during the Photo-Fenton process may speculatively be explained as follows; the most important source of $HO^{\cdot}$ is the direct reaction between $Fe^{2+}$ and $H_2O_2$ (dark Fenton's reaction) for both Fenton and Photo-Fenton processes. Since during the initial stages of the Photo-Fenton reaction $H_2O_2$ is not only consumed via dark Fenton but also via UV-C photolysis (though significantly less due to the high UV-C absorbance of K-acid), less $H_2O_2$ is available for the direct Fenton's reaction, that initially may retard the oxidation reaction [34].

Another reason for the retardation in TOC abatement rates might be that the initial formation rate of $HO^{\cdot}$ radicals in the Photo-Fenton system is so high that many $HO^{\cdot}$ are consumed via side reactions with $H_2O_2$ and $HO_2^-$ [35].

At the end of the 120 min treatment period, COD and TOC removals were obtained as 30% ($H_2O_2$/UV-C-control), 61% (dark Fenton-control) and 93% (Photo-Fenton process) as well as 11% ($H_2O_2$/UV-C-control), 38% (dark Fenton-control) and 95% (Photo-Fenton process), respectively. Considering that $H_2O_2$/UV-C as well as dark Fenton treatment of this commercially important naphthalene sulfonate resulted in very poor and/or incomplete oxidation,

**Table 4**
ANOVA results for the experimental design of K-acid Photo-Fenton oxidation in terms of percent parent pollutant (K-acid) and organic matter (COD, TOC) removal efficiencies.

| Output | K-acid removal | | | COD removal | | | TOC removal | | |
|---|---|---|---|---|---|---|---|---|---|
| | SS[a] | *F*-Value | Prob > *F* | SS[a] | *F*-Value | Prob > *F* | SS[a] | *F*-Value | Prob > *F* |
| Model | 2753.62 | 18.17 | <0.0001 | 8523.62 | 8.33 | 0.0006 | 17747.17 | 8.40 | 0.0006 |
| $X_1$ | 1214.10 | 112.18 | <0.0001 | 893.04 | 12.22 | 0.0050 | 2044.26 | 13.54 | 0.0036 |
| $X_2$ | 986.63 | 91.16 | <0.0001 | 3322.91 | 45.46 | <0.0001 | 8306.76 | 55.03 | <0.0001 |
| $X_3$ | 104.58 | 9.66 | 0.0100 | 2064.62 | 28.24 | 0.0002 | 3702.65 | 24.53 | 0.0004 |
| $X_4$ | 326.34 | 30.15 | 0.0002 | 408.38 | 5.59 | 0.0376 | 446.34 | 2.96 | 0.1135 |
| $X_1 \times X_2$ | 7.70 | 0.71 | 0.4169 | 144.00 | 1.97 | 0.1880 | 363.86 | 2.41 | 0.1488 |
| $X_1 \times X_3$ | 1.27 | 0.12 | 0.7388 | 28.09 | 0.38 | 0.5479 | 112.89 | 0.75 | 0.4056 |
| $X_1 \times X_4$ | 15.80 | 1.46 | 0.2523 | 144.00 | 1.97 | 0.1880 | 193.91 | 1.28 | 0.2811 |
| $X_2 \times X_3$ | 0.95 | 0.088 | 0.7725 | 333.06 | 4.56 | 0.0561 | 1546.46 | 10.25 | 0.0084 |
| $X_2 \times X_4$ | 15.41 | 1.42 | 0.2579 | 8.12 | 0.11 | 0.7451 | 47.27 | 0.31 | 0.5870 |
| $X_3 \times X_4$ | $6.25 \times 10^{-4}$ | $5.77 \times 10^{-5}$ | 0.9941 | 0.42 | $5.78 \times 10^{-3}$ | 0.9408 | 27.30 | 0.18 | 0.6788 |
| $X_1^2$ | 60.49 | 5.59 | 0.0375 | 286.30 | 3.92 | 0.0734 | 584.85 | 3.87 | 0.0747 |
| $X_2^2$ | 0.17 | 0.015 | 0.9033 | 18.79 | 0.26 | 0.6222 | 135.73 | 0.90 | 0.3634 |
| $X_3^2$ | 2.96 | 0.27 | 0.6115 | 831.01 | 11.37 | 0.0062 | 203.39 | 1.35 | 0.2703 |
| $X_4^2$ | 20.61 | 1.90 | 0.1950 | 0.39 | $5.37 \times 10^{-3}$ | 0.9429 | 12.95 | 0.086 | 0.7750 |

[a] Sum of squares.

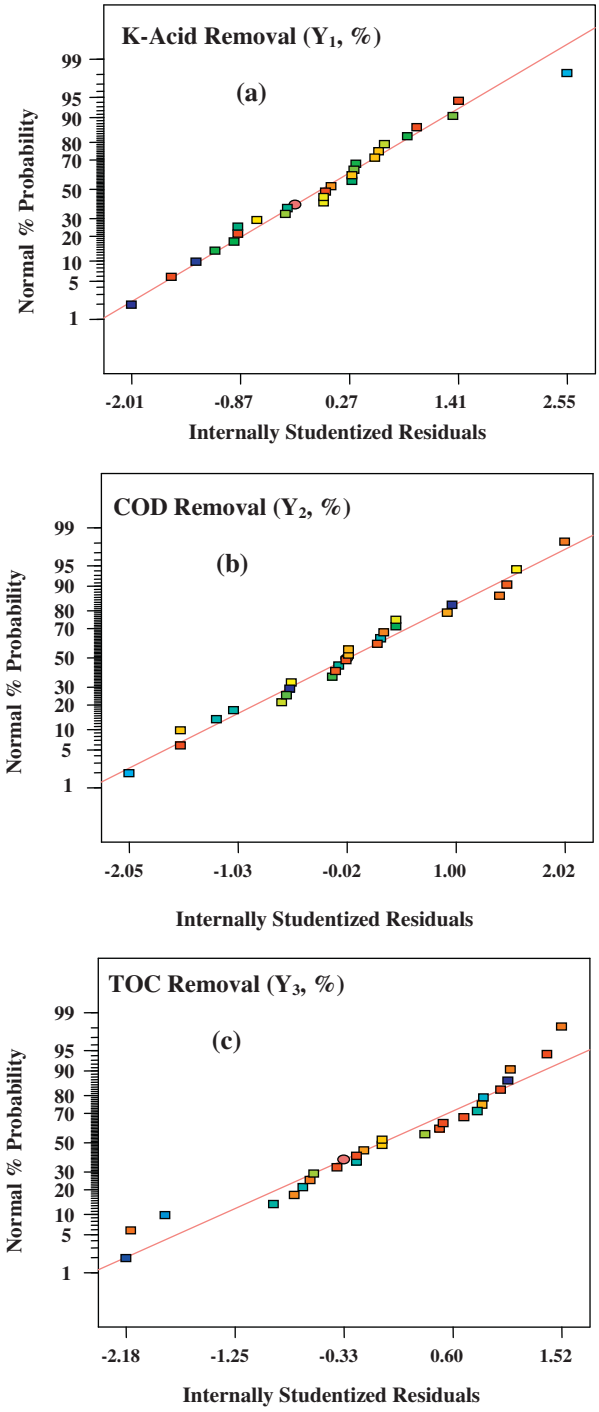


**Fig. 2.** The internally studentized residuals and normal % probability plots established for K-acid, COD and TOC removals.

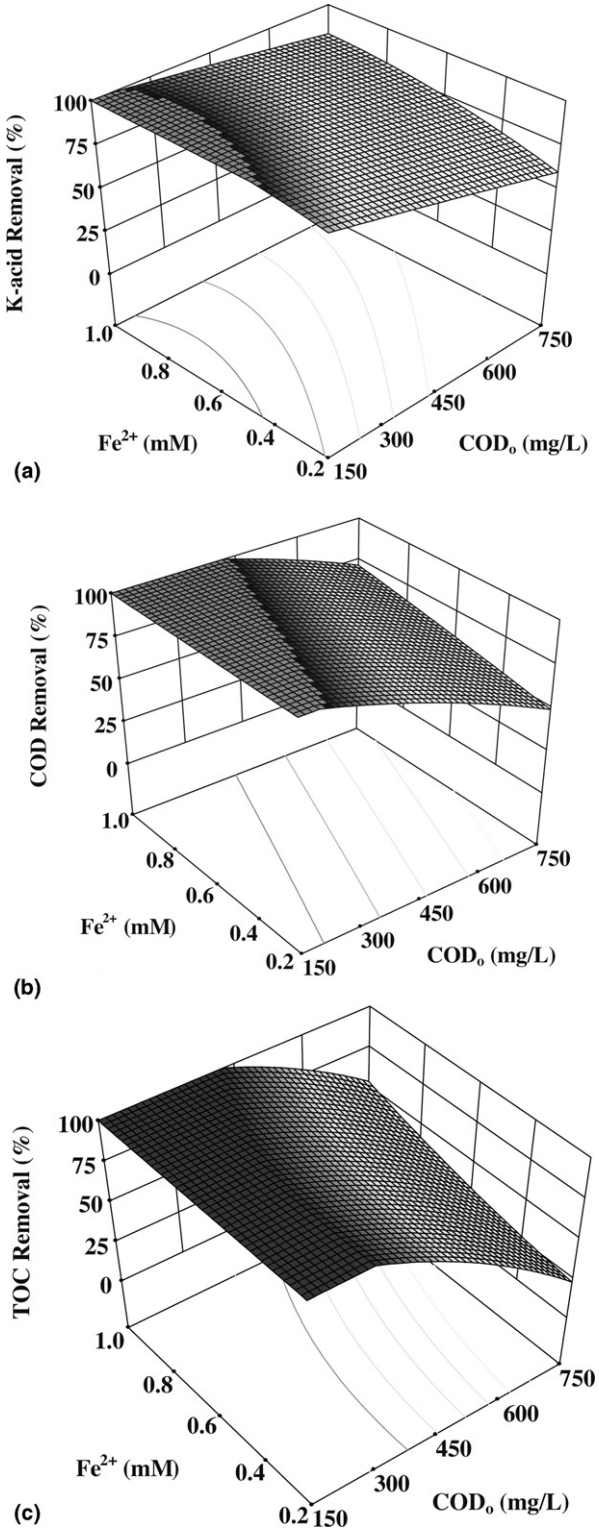


**Fig. 3.** 3-D plots obtained for Photo-Fenton oxidation of aqueous K-acid solution: Elucidation of the combined effect of $Fe^{2+}$ and $COD_0$ of K-acid on K-acid (a), COD (b) and TOC (c) removal efficiencies. Experimental conditions: $H_2O_2$ = 30 mM; $t_r$ = 30 min for K-acid and $t_r$ = 75 min for COD and TOC removals.

UV-C light-assisted Fenton oxidation appears to be a more suitable option for the treatment of aqueous K-acid solutions.

### 3.2. Photo-Fenton treatment of aqueous K-acid: process optimization

Experimentally obtained results (percent K-acid, COD and TOC removal efficiencies) of the design matrix with probable error ranges are presented in Table 3 together with the predicted responses obtained from polynomial regression equations. As is obvious from Table 3, experimental and model results were in most cases compatible with each other.

The Design Expert® software generated the following polynomial regression equations which demonstrate the empirical relationship between $t_r$ ($X_1$), initial COD ($X_2$), $H_2O_2$ ($X_3$) and $Fe^{2+}$ ($X_4$) concentrations and responses of K-acid ($Y_1$), COD ($Y_2$) and TOC

**Table 5**
Experimentally obtained and predicted K-acid, COD and TOC removal efficiencies at local optimum (varying initial COD) values.

| $COD_o$ (mg/L) – target | $t_r$ (min) | $H_2O_2$ (mM) | $Fe^{2+}$ (mM) | K-acid removal (%) | | COD removal (%) | | TOC removal (%) | |
|---|---|---|---|---|---|---|---|---|---|
| | | | | Model | Experimental | Model | Experimental | Model | Experimental |
| 150-FO[a] | 51 | 37.7 | 0.7 | 100 | 95 ± 5 | 100 | 95 ± 5 | 100 | 94 ± 6 |
| 300-FO | 58 | 30.7 | 0.7 | 100 | 95 ± 5 | 100 | 99 ± 1 | 97 | 91 ± 9 |
| 450-FO | 83 | 37.5 | 0.8 | 100 | 95 ± 5 | 97 | 95 ± 5 | 100 | 97 ± 3 |
| 450-PO[b] | 55 | 20.0 | 0.4 | 90 | 95 ± 5 | 60 | 74 ± 7 | 55 | 48 ± 5 |
| 600-PO | 62 | 34.2 | 0.4 | 100 | 96 ± 4 | 69 | 74 ± 7 | 55 | 56 ± 6 |
| 750-PO | 75 | 38.5 | 0.6 | 100 | 95 ± 5 | 73 | 78 ± 8 | 61 | 65 ± 7 |

[a] Full (complete) oxidation target.
[b] Partial oxidation target (complete K-acid abatement and meeting the discharge limit of <200 mg/L COD).

($Y_3$) removal efficiencies in terms of coded factors;

$$Y_1(\%) = 89.60 + 7.11 \times X_1 - 6.41 \times X_2 + 2.09 \times X_3 + 3.69 \times X_4 + 0.69 \times X_1 \times X_2 - 0.99 \times X_1 \times X_4 + 0.28 \times X_1 \times X_3 + 0.98 \times X_2 \times X_4 - 0.24 \times X_2 \times X_3 - 6.250 \times 10^{-3} \times X_4 \times X_3 - 1.86 \times (X_1)^2 - 0.098 \times (X_2)^2 - 0.41 \times (X_3)^2 - 1.09 \times (X_4)^2 \quad (R^2 = 0.9586) \tag{3}$$

$$Y_2(\%) = 89.50 + 6.10 \times X_1 - 11.77 \times X_2 + 9.28 \times X_3 + 4.13 \times X_4 + 3.00 \times X_1 \times X_2 - 3.00 \times X_1 \times X_4 + 1.32 \times X_1 \times X_3 + 0.71 \times X_2 \times X_4 + 4.56 \times X_2 \times X_3 - 0.16 \times X_3 X_4 - 4.05 \times (X_1)^2 - 1.04 \times (X_2)^2 - 6.90 \times (X_3)^2 - 0.15 \times (X_4)^2 \quad (R_2 = 0.9138) \tag{4}$$

$$Y_3(\%) = 84.40 + 9.23 \times X_1 - 18.60 \times X_2 + 12.42 \times X_3 + 4.31 \times X_4 + 4.77 \times X_1 \times X_2 + 2.66 \times X_1 \times X_3 - 3.48 \times X_1 \times X_4 + 1.72 \times X_2 \times X_4 + 9.83 \times X_2 \times X_3 + 1.31 \times X_3 \times X_4 - 5.79 \times (X_1)2 - 2.79 \times (X_2)^2 - 3.41 \times (X_3)^2 + 0.86 \times (X_4)^2 \quad (R^2 = 0.9145) \tag{5}$$

$(-2 \le X_i \le 2)$

The factors in front of the coded model terms indicate the intensity and direction (positive or negative) of the influence of that process independent variable on the response (see Eqs. (3)–(5)). A positive effect of a factor means that the response is improved when the factor level increases and a negative effect of the factor revealed that the response is inhibited when the factor level increases [36]. For instance, from Eq. (3) it is evident that the variable "$t_r$" ($X_1$) exhibited the highest positive influence on percent K-acid removal, whereas the variable "$H_2O_2$ concentration" ($X_3$) had the highest positive impact on COD and TOC abatements. The strongest negative effect on K-acid, COD and TOC removals was found as the initial COD content ($X_2$) of the K-acid solutions. According to the established second-order regression models, the decreasing order of the influence of process independent variables on K-acid removal efficiency was $t_r$ > $COD_o$ (negative impact) > $Fe^{2+}$ > $H_2O_2$, and $COD_o$ (negative impact) > $H_2O_2$ > $t_r$ > $Fe^{2+}$ in terms of COD and TOC removal efficiencies. The above mentioned rankings among the examined process independent variables imply that the factors influencing parent compound and organic matter degradation may differ significantly from each other. For instance, it is completely reasonable that the variable $t_r$ has more impact on K-acid degradation, which disappeared at a faster rate, than on COD and TOC removals, whereas the oxidant ($H_2O_2$) concentration plays a more important role in organic matter degradation that is harder to achieve than parent compound removal. In a similar manner, Ay et al. [19] concluded on the basis of the coefficients determined by their Box–Behnken design that color removal efficiency decreased with increasing initial dyestuff concentration and increased at elevated $H_2O_2$ and $Fe^{2+}$ concentrations. Rozas et al. [37] applied a circumscribed CCD to model and optimize the degradation of the antibiotic ampicillin by Fenton and Photo-Fenton processes. They concluded that the variables pH and $Fe^{2+}$ concentration had by far more influence on antibiotic removal than the other studied parameters. Masomboon et al. [38] employed the Box–Behnken design tool to examine the degradation of o-toluidine by the Photo-Fenton process. According to their findings, $H_2O_2$ and $Fe^{2+}$ concentrations were the main parameters affecting o-toluidine and COD abatements.

Table 4 displays the ANOVA results for the full second-order polynomial regression models generated for removal of K-acid, COD and TOC with the Photo-Fenton process oxidation at 95% confidence levels. The correctness and fitness of the models were examined by the $R^2$ found as 0.9586, 0.9138 and 0.9145 for K-acid, COD and TOC removals, respectively. From their values it is evident that 95.86%, 91.38% and 91.45% of the variability in the responses could be explained by the regression models. According to the ANOVA, the model *F*-values determined as 18.17, 8.33 and 8.40, as well as Prob > *F*-values that were less than 0.0001, 0.0006 and 0.0006 for K-acid, COD and TOC removals, respectively, the model terms were significant (Table 4). The adequate precision values of the models compare the predicted data at the design points with the average prediction error. In other words, it measures the signal-to-noise ratio [22]. A ratio greater than 4 is desirable for an appropriate model. In the present study, the adequate precision values were obtained as 15.45, 11.23 and 10.46 for K-acid, COD and TOC removals, respectively. These values indicate an adequate signal and suggest that the regression models can be used to navigate the design space for Photo-Fenton oxidation of K-acid. As can be seen from the Prob > *F*-values and *F*-values presented in Table 4, the most important terms are the linear ones (reaction time, initial COD, $H_2O_2$ and $Fe^{2+}$ concentrations). Although the full models showed a significant fit, some terms, namely the interaction and quadratic terms, could be considered as insignificant for the full model on the basis of Prob > *F*-values that were higher than 0.10 [36]. However, since the "adjusted *R*-squared" values (0.9058 for K-acid, 0.8041 for COD and 0.8056 for TOC responses) were in reasonable agreement with the $R^2$ values, all terms were included in the models [39]. Besides, excluding these terms from the models would have been reduced the $R^2$ values to 0.9353, 0.8755 and 0.8546 for K-acid, COD and TOC removals, respectively. On the other hand, "adjusted *R*-squared" values remained approximately at the same level (0.9191 for K-acid, 0.8271 for COD and 0.8087 for TOC responses).

The diagnostic plots (Fig. 2) imply that the assumptions of normality, independence and randomness of the residuals (i.e. the difference between the observed and predicted or fitted values of each process response) are all satisfied. In Fig. 2, residuals show how well the models satisfy the ANOVA assumptions where the studentized residuals measure the number of standard deviations by separating the actual and predicted values from one another [22,40]. Fig. 2 also implies that a response transformation was not required and there was no apparent problem with normality.

### 3.3. Evaluation of combined effects of $Fe^{2+}$ concentration and initial COD on Photo-Fenton oxidation of aqueous K-acid

Fig. 3 displays the 3-D plots generated for Photo-Fenton oxidation of aqueous K-acid solution in terms of K-acid (a), COD (b) and TOC (c) removal efficiencies by the Design-Expert® software. In the present study it was decided to focus on the dual effect of the parameters "$COD_o$" and "$Fe^{2+}$" on the treatment efficiencies for further assessment and elucidation. 3-D surface plots were established for a fixed initial $H_2O_2$ concentration of 30 mM and a treatment time of 30 min to present combinative effects on K-acid removal efficiencies. From Fig. 3(a) it is evident that a K-acid removal of ≥95% could only be achieved for $COD_o$ values ≤450 mg/L and K-acid abatement decreased dramatically with increasing $COD_o$ from 100% to 80–85%, even at the highest applied $Fe^{2+}$ concentration (1.0 mM). In order to ensure high K-acid removals (95–100%), the $Fe^{2+}$ concentration had to be increased from its lowest value (0.2 mM) to 0.6 mM for a $COD_o$ value of 300 mg/L and to 1.0 mM for a $COD_o$ range of 300–450 mg/L.

The negative influence of increasing the $COD_o$ of aqueous K-acid solution on Photo-Fenton treatment performance was more pronounced in terms of the parameters COD and TOC. For the 3-D graphs presenting the binary impact of the process variables $COD_o$ and $Fe^{2+}$ on organic matter removal, $H_2O_2$ concentration was again kept constant at 30 mM but $t_r$ was elevated to 75 min. The removal trends observed for the parameters COD and TOC were similar to those observed for K-acid but removal efficiencies dropped more intensely. For instance, for the highest $COD_o$ value (750 mg/L), COD removal efficiencies that were obtained in the range of 48–49% in the presence of 0.2 mM $Fe^{2+}$ increased to 72–73% in the presence of 1.0 mM added $Fe^{2+}$. Obviously, increasing the photocatalyst concentration from 0.2 to 1.0 mM resulted in a significant enhancement in terms of K-acid and organic matter abatement rates. On the other hand, TOC removal efficiencies dropped dramatically beyond a $COD_o$ of 450 mg/L, above value complete mineralization could never be achieved even at the highest studied $Fe^{2+}$ concentration. Apparently, the observed treatment efficiencies were also affected by the parameter "initial $H_2O_2$ concentration" that had a significant positive effect particularly on TOC abatement in the range of 20–40 mM (data not shown). From the graphical presentations derived for Photo-Fenton treatment of aqueous K-acid solution it is obvious that, in parallel to the above statistical evaluations, TOC is the "hardest" (most difficult-to-remove) parameter among the selected process responses thus requiring harsher reaction conditions ($Fe^{2+}$, $H_2O_2$ concentrations and/or $t_r$) to mineralize K-acid degradation products.

### 3.4. Optimization of Photo-Fenton treatment of aqueous K-acid

Table 5 summarizes the experimental conditions (optimized in terms of $t_r$, $H_2O_2$ and $Fe^{2+}$ concentrations) required to achieve the targeted treatment efficiencies at varying $COD_o$ values of K-acid solution called local optima. The treatment targets were, as aforementioned (i) FO, for stand-alone, full treatment of K-acid producing effluents via Photo-Fenton process, or alternatively, and (ii) PO, i.e. partial oxidation, in order to completely eliminate the recalcitrant parent pollutant and to comply with the national legislations for discharge into receiving water bodies [41]. According to the Turkish Water Pollution Control Regulation (WPCR), the maximum allowable discharge limit value for the COD parameter is 200 mg/L and to be on the safe side (in cases of emergencies or technical problems), the desired removal efficiency for the optimization procedure was adjusted as to reduce the COD value to at least 180 mg/L. Table 5 also presents achievable treatment goals and options foreseen by the established regression models for K-acid, COD and TOC removals together with the experimentally obtained treatment efficiencies. Upon comparison of the predicted and observed removal rates it is evident that the values obtained for the foreseen treatment targets were close to each other. It should also be noted here that the "FO" target was not achievable at the higher $COD_o$ values (600 and 750 mg/L), even upon increase of treatment time, catalyst and/or oxidant concentrations. Hence, for these two elevated $COD_o$ values, only the "PO" treatment goal (namely complete K-acid removal and partial organic matter oxidation) could be satisfactorily fulfilled under the studied reaction conditions. Again, the dramatic reduction in treatment efficiencies is obvious for $COD_o$ values beyond 450 mg/L. When the $COD_o$ was

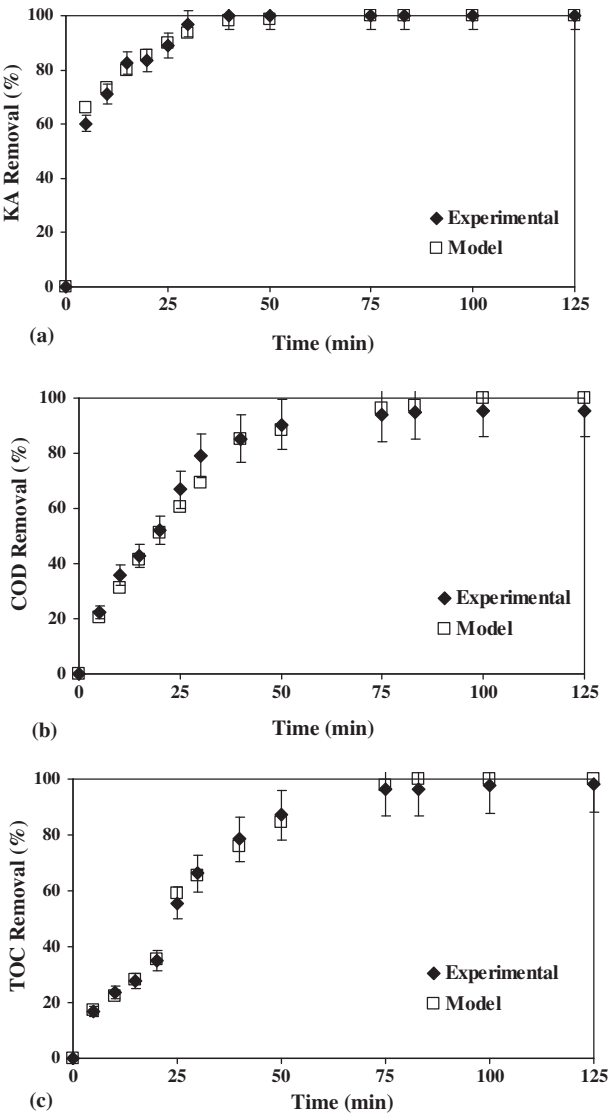


**Fig. 4.** Experimental and predicted K-acid (a), COD (b) and TOC (c) removals as a function of Photo-Fenton treatment time for the locally optimized treatment target "*Full Oxidation* (*FO*)". Experimental conditions: $COD_o$: 450 mg/L; K-acid = 791 mg/L; TOC = 155 mg/L; $H_2O_2$: 37.5 mM; $Fe^{2+}$ = 0.8 mM; initial pH 3.0.

450 mg/L, both treatment options (FO, PO goals) were still applicable and as elucidated in Table 5. From Table 5 the considerably "milder" reaction condition (i.e. the relatively low $H_2O_2$ and $Fe^{2+}$ concentrations as well as short $t_r$ values) foreseen for the partial treatment goals ($COD_o$ = 450, 600 and 750 mg/L) are also obvious.

Fig. 4 elucidates experimentally obtained and modeled (predicted) K-acid (a), COD (b) and TOC (c) removal efficiencies as a function of Photo-Fenton treatment time. In order to avoid confusion, only the results for the optimization of the FO treatment target at $COD_o$ = 450 mg/L were exemplified. From Fig. 4 it can be seen that K-acid degradation is relatively fast and complete after 25–30 min treatment, whereas practically full oxidation is achieved after 75–80 min in terms of the parameters COD and TOC. It should also be emphasized herein that although K-acid removal efficiencies were modeled for a treatment period of 0–50 min and for organic matter (COD and TOC) removals a reaction time ranging between 25 and 125 min was considered, the experimental data and corresponding predicted treatment results were presented for the entire Photo-Fenton treatment time (0–125 min). Fig. 4 implies that the removal efficiencies calculated by using the regression models fell within the ranges of the experimentally obtained Photo-Fenton treatment results, even beyond the studied treatment periods. Hence, from Fig. 4 it can be deduced that the regression models generated for Photo-Fenton oxidation of K-acid and its degradation products were capable of accurately predicting treatment results and thus can even be used for safely extrapolating treatment results for varying photocatalytic treatment periods.

## 4. Concluding remarks

In the present study, Photo-Fenton treatment of K-acid and its organic degradation products was separately modeled and optimized using multivariate analysis. The following conclusions could be drawn from the present study:

- Ranges of the independent process variables should be chosen very carefully in order to establish models that are capable of accurately predicting Photo-Fenton oxidation of K-acid and its organic carbon content. In the present study the selected process parameter ranges were all appropriates and could be used to establish statistically sound and reliable experimental design models.
- The experimentally obtained and predicted results were highly comparable for all selected treatment targets at different initial COD values as well as throughout the entire photocatalytic treatment period up to 125 min.
- From the established polynomial regression models it was evident that the initial COD of the K-acid solution had a significant negative effect on treatment performance, whereas all the other process independent variables had a positive influence on treatment efficiencies. Photo-Fenton treatment was mostly affected by the two process variables "initial COD" and "treatment time".
- For initial COD values > 450 mg/L (600 and 750 mg/L), only partial oxidation could be achieved even under the harshest investigated reaction conditions, whereas complete removal of the selected process responses was possible for initial COD values ≤ 450 mg/L (150, 300 and 450 mg/L).

## Acknowledgements

The authors acknowledge the financial support of the Scientific and Technological Research Council of Turkey (TUBITAK) under project number 108Y051 and Eksoy Chemicals for the K-acid samples.

## References

[1] I. Arslan-Alaton, T. Olmez-Hanci, Biological, chemical and photochemical treatment of commercially important naphthalene sulphonates, in: D. Fatta-Kassinos, K. Bester, K. Kümmerer (Eds.), Xenobiotics in the Urban Water Cycle, Springer, Heidelberg, 2010, pp. 413–430.
[2] B. Altenbach, W. Giger, Determination of benzene- and naphthalenesulfonates in wastewater by solid-phase extraction with graphitized carbon black and ion-pair liquid chromatography with UV detection, Anal. Chem. 67 (1995) 2325–2333.
[3] M. Sanchez-Polo, J. Rivera-Utrilla, C.A. Zaror, Advanced oxidation with ozone of 1,3,6-naphthalenetrisulfonic acid in aqueous solution, J. Chem. Technol. Biotechnol. 77 (2002) 148–154.
[4] M. Sanchez-Polo, J. Rivera-Utrilla, J.D. Mendez-Diaz, S. Canonica, U. von Gunten, Photooxidation of naphthalenesulfonic acids: comparison between processes based on $O_3$, $O_3$/activated carbon and UV/$H_2O_2$, Chemosphere 68 (2007) 1814–1820.
[5] H. De Wever, S. Weiss, T. Reemtsma, J. Vereecken, J. Müller, T. Knepper, O. Rörden, S. Gonzalez, D. Barcelo, M.D. Hernando, Comparison of sulfonated and other micropollutants removal in membrane bioreactor and conventional wastewater treatment, Water Res. 41 (2007) 935–945.
[6] O. Legrini, E. Oliveros, A.M. Braun, Photochemical processes for water treatment, Chem. Res. 93 (1993) 671–698.
[7] E. Oliveros, O. Legrini, M. Hohl, T. Müller, A.M. Braun, Industrial wastewater treatment: large-scale development of a light-enhanced Fenton reaction, Chem. Eng. Process. 36 (1997) 397–405.
[8] I. Arslan-Alaton, T. Olmez-Hanci, B.H. Gursoy, G. Tureli, $H_2O_2$/UV-C treatment of the commercially important aryl sulfonates H-, K-, J-acid and para base: assessment of photodegradation kinetics and products, Chemosphere 76 (2009) 587–594.
[9] I. Arslan-Alaton, N. Ayten, T. Olmez-Hanci, Photo-Fenton-like treatment of the commercially important H-acid: process optimization by factorial design and effects of photocatalytic treatment on activated sludge inhibition, Appl. Catal. B: Environ. 96 (2010) 208–217.
[10] J. De Laat, H. Gallard, S. Ancelin, B. Legube, Comparative study of the oxidation of atrazine and acetone by $H_2O_2$/UV, Fe(III)/UV, Fe(III)/$H_2O_2$/UV and Fe(II) or Fe(III)/$H_2O_2$, Chemosphere 39 (1999) 2693–2706.
[11] M. Perez, F. Torrades, X. Domenech, J. Peral, Fenton and photo-Fenton oxidation of textile effluents, Water Res. 36 (2002) 2703–2710.
[12] S. Parsons, M. Williams, Advanced Oxidation Processes for Water and Wastewater Treatment, IWA Publishing, London, 2004 (Chapters 1 and 5).
[13] J.J. Pignatello, Dark and photo-assisted $Fe^{3+}$ catalyzed degradation of chlorophenoxy herbicides by hydrogen peroxide, Environ. Sci. Technol. 26 (1992) 944–951.
[14] G. Ruppert, R. Bauer, G. Heisler, The photo-Fenton reaction – an effective photochemical wastewater treatment process, J. Photochem. Photobiol. A 73 (1993) 75–78.
[15] M. Muruganandham, M. Swaminathan, Decolourisation of reactive orange 4 by Fenton and photo-Fenton oxidation technology, Dyes Pigments 63 (2004) 315–321.
[16] L. Nunez, J.A. Garcia-Hortal, F. Torrades, Study of kinetic parameters related to the decolourization and mineralization of reactive dyes from textile dyeing using Fenton and photo-Fenton processes, Dyes Pigments 75 (2007) 647–652.
[17] M.S. Secula, G.D. Suditu, I. Poulios, C. Cojocaru, I. Cretescu, Response surface optimization of the photocatalytic decolorization of a simulated dyestuff effluent, Chem. Eng. J. 141 (2008) 18–26.
[18] I. Arslan-Alaton, G. Tureli, T. Olmez-Hanci, Treatment of azo dye production wastewaters using Photo-Fenton-like advanced oxidation processes: optimization by response surface methodology, J. Photochem. Photobiol. A 202 (2009) 142–153.
[19] F. Ay, E. Cokay Catalkaya, F. Kargi, A statistical experiment design approach for advanced oxidation of direct red azo-dye by photo-Fenton treatment, J. Hazard. Mater. 162 (2009) 230–236.
[20] M.J. Anderson, P.J. Whitcomb, RSM Simplified: Optimizing Processes Using Response Surface Methods for Design of Experiments, Productivity Press, New York, 2005.
[21] D. Bas, I.H. Boyaci, Modeling and optimization I: usability of response surface methodology, J. Food Eng. 78 (2007) 836–845.
[22] R.H. Myers, D.C. Montgomery, C.M. Anderson-Cook, Response Surface Methodology: Process and Product Optimization Using Designed Experiments, third ed., John Wiley, Inc., New Jersey, 2009.
[23] I. Nicole, J. de Laat, M. Dore, J.P. Duguet, C. Bonnel, Use of UV radiation in water treatment: measurement of photonic flux by hydrogen peroxide actinometry, Water Res. 24 (1990) 157–168.
[24] T. Oppenländer, Photochemical Purification of Water and Air: Advanced Oxidation Processes (AOPs): Principles, Reaction Mechanisms, Reactor Concepts, John Wiley, Inc., Chichester, 2003.
[25] B.K. Körbahti, Response surface optimization of electrochemical treatment of textile dye wastewater, J. Hazard. Mater. 145 (2007) 277–286.
[26] M.A. Rauf, N. Marzoukia, B.K. Körbahti, Photolytic decolorization of rose bengal by UV/$H_2O_2$ and data optimization using response surface method, J. Hazard. Mater. 159 (2008) 602–609.
[27] T. Olmez, The optimization of Cr(VI) reduction and removal by electrocoagulation using response surface methodology, J. Hazard. Mater. 162 (2009) 1371–1378.

[28] B.K. Körbahti, M.A. Rauf, Determination of optimum operating conditions of carmine decoloration by UV/$H_2O_2$ using response surface methodology, J. Hazard. Mater. 161 (2009) 281–286.
[29] ISO 6060, Water Quality-Determination of the Chemical Oxygen Demand, second ed., ISO 6060/TC 147, Geneva, 1989.
[30] Official Methods of Analysis, Association of Official Anal. Chemist., Washington, DC, 1980.
[31] K. Swaminathan, K. Pachhade, S. Sandhya, Decomposition of a dye intermediate 1 amino-8 naphthol-3,6 disulphonic acid (H-acid) in aqueous solution by ozonation, Desalination 186 (2005) 155–164.
[32] A. Socha, E. Chrzescijanska, E. Kusmierek, Photoelectrochemical treatment of H-acid at electrode covered with $TiO_2$/$RuO_2$, Dyes Pigments 71 (2006) 10–18.
[33] M. Yang, J. Hu, K. Ito, Characteristics of $Fe^{2+}$/$H_2O_2$/UV oxidization process, Environ. Technol. 19 (1998) 183–191.
[34] Y.F. Sun, J.J. Pignatello, Photochemical-reactions involved in the total mineralization of 2,4-D by $Fe^{3+}$/$H_2O_2$/UV, Environ. Sci. Technol. 27 (1993) 304–310.
[35] M.I. Stefan, A.R. Hoy, J.R. Bolton, Kinetics and mechanism of the degradation and mineralization of acetone in dilute aqueous solution sensitized by the UV photolysis of hydrogen peroxide, Environ. Sci. Technol. 30 (1996) 2382–2390.
[36] K. Cruz-González, O. Tores-Lopez, A. Garcia-Leon, J.L. Guzman-Mar, L.H. Reyes, A. Hernandez-Ramirez, J.M. Peralta-Herandez, Determination of optimum parameters for Acid Yellow 36 decolorization by electro-Fenton process using BDD cathode, Chem. Eng. J. 160 (2010) 199–206.
[37] O. Rozas, D. Contreras, M.A. Mondaca, M. Pérez-Moya, H.D. Mansilla, Experimental design of Fenton and photo-Fenton reactions for the treatment of ampicillin solutions, J. Hazard. Mater. 177 (2010) 1025–1030.
[38] N. Masomboon, C.-W. Chen, J. Anotai, M.-C. Lu, A statistical experimental design to determine o-toluidine degradation by the photo-Fenton process, Chem. Eng. J. 159 (2010) 116–122.
[39] C. Hong, W. Haiyun, Optimization of volatile fatty acid production with co-substrate of food wastes and dewatered excess sludge using response surface methodology, Bioresour. Technol. 101 (2010) 5487–5493.
[40] A. Özer, G. Gürbüz, A. Calimli, B.K. Körbahti, Biosorption of copper(II) ions on *Enteromorpha prolifera*: application of response surface methodology (RSM), Chem. Eng. J. 146 (2009) 377–387.
[41] Turkish WPCR, Official Newspaper Ref. Nr. 25687 dated 31 December 2004, Ankara.